Differential role of Rab proteins in ciliary trafficking: Rab23 regulates Smoothened levels

Christopher Boehlke[1,*], Mikhail Bashkurov[1,*,‡], Andrea Buescher[1], Theda Krick[1], Anne-Katharina John[1], Roland Nitschke[2,3], Gerd Walz[1,3] and E. Wolfgang Kuehn[1,§]

[1]Renal Unit, University Medical Center, University of Freiburg, Hugstetter Strasse 55, Freiburg, 79106 Germany
[2]Life Imaging Center, Center for Biological Systems Analysis, Albert-Ludwig-University of Freiburg, Habsburgerstrasse 49, 79104 Freiburg, Germany
[3]Center for Biological Signalling Studies (bioss), Albertstrasse 94, 79104 Freiburg, Germany

*These authors contributed equally to this work
‡Present address: Samuel Lunenfeld Research Institute, 600 University Avenue, Toronto, ON, M5G 1X5, Canada
§Author for correspondence (wolfgang.kuehn@uniklinik-freiburg.de)

Accepted 11 February 2010
Journal of Cell Science 123, 1460-1467

doi:10.1242/jcs.058883

Summary

The structure and function of the primary cilium as a sensory organelle depends on a motor-protein-powered intraflagellar transport system (IFT); defective IFT results in retinal degeneration and pleiotropic disorders such as the Bardet Biedl syndrome (BBS) and defective hedgehog (HH) signaling. Protein transport to the cilium involves Rab GTPases. Rab8, together with a multi protein complex of BBS proteins, recruits cargo to the basal body for transport to the cilium. Loss of Rab23 in mice recapitulates the HH phenotype but its function in HH signaling is unknown. Here we established a novel protocol, based on fluorescence recovery after photo-bleaching (FRAP), allowing the quantitative analysis of protein transport into the cilium of MDCK cells. We compared the effect of Rab8, Rab5 and Rab23 on the ciliary transport of the HH-associated transmembrane receptor Smoothened, the microtubular tip protein EB1, and the receptor protein Kim1. Ciliary FRAP confirmed the role of Rab8 in protein entry to the cilium. Dominant negative Rab5 had no impact on the ciliary transport of Smoothened or EB1, but slowed the recovery of the apical protein Kim1 in the cilium. Depletion of Rab23 or expression of dominant-negative Rab23 decreased the ciliary steady state specifically of Smoothened but not EB1 or Kim1, suggesting a role of Rab23 in protein turnover in the cilium.

Key words: EB1, FRAP, IFT, Kim1, Cilia, Smoothened

Introduction

Primary cilia are filiform structures protruding from the plasma membrane that have been tied to a broad range of genetic disorders (Singla and Reiter, 2006). The cilium is anchored to the apical plasma membrane by the basal body, a structure derived from the mother centriole. Transition fibers connect the basal body with the plasma membrane, separating the ciliary compartment from the cytosol (Rosenbaum and Witman, 2002). Nine microtubule doublets extend from the basal body to build the axoneme which is covered by a membranous sheath that is continuous with the plasma membrane. The ciliary architecture is established and maintained by an intraflagellar transport (IFT) system. Cargo proteins, linked to IFT particles, are transported by the microtubular motor kinesin II to the tip of the cilium (anterograde transport) where they are transferred to dynein (Pedersen et al., 2008). Retrograde transport carries cargo back to the base of the cilium and the cytoplasm, where it is then believed to be recycled. This transport mechanism is essential for the structure and function of cilia, since targeted disruption of IFT proteins or kinesin II subunits such as Kif3A in mice result in the loss of cilia and phenotypes resembling human genetic ciliopathies (Lin et al., 2003; Taulman et al., 2001; Yoder et al., 2002).

In rod photoreceptors at the retina, which are modified cilia (Roepman and Wolfrum, 2007), the transport of rhodopsin through the connecting cilium begins with the fusion of Golgi-derived rhodopsin-containing vesicles with specified subdomains of the plasma membrane near the base of the cilium (Maerker et al., 2008). Specificity of vesicular transport to subcellular compartments is controlled by GTPases of the Rab family (Grosshans et al., 2006). Biochemical analysis of photoreceptors identified Rab3, -6, -8A and -11 as components of the rhodopsin-containing vesicles, suggesting that rhodopsin is transported in a Rab-dependent manner (Deretic, 1997). Subsequently it was shown that constitutive expression of a dominant-negative form of Rab8a lead to retinal degeneration (Moritz et al., 2001), confirming the role of Rab8 in the transport of rhodopsin through the connecting cilium to the outer segment of photoreceptors. Two recent studies uncovered the crucial role of Rab8a-dependent vesicular traffic for the formation of primary cilia. In a screen analyzing 39 GTPase-activating proteins (GAPs), Rab8a, -17 and -23 were essential for ciliogenesis, but only Rab8a was present in the cilium (Yoshimura et al., 2007). Neither Rab17 nor Rab23 was detected in the cilium, although Rab23 was previously recognized as a negative regulator of hedgehog (HH) signaling, which is an IFT-dependent pathway (Eggenschwiler et al., 2006). Nachury et al. found that the Rab8 guanine exchange factor (GEF) Rabin8 interacts with a multi-protein complex of seven Bardet Biedl syndrome (BBS) proteins (Nachury et al., 2007), and proposed that the multimeric BBS protein complex recruits Rab8 via its GEF, Rabin8, to direct post-Golgi vesicles to fuse with the plasma membrane near the ciliary base.

The study of protein transport into mammalian cilia, where important pathways such as the HH and Wnt pathway rely on IFT for their action (Scholey and Anderson, 2006), has been limited by the availability of readouts. Impaired cilia formation was used to implicate proteins in transport to the cilium (Follit et al., 2006; Nachury et al., 2007; Yoshimura et al., 2007). The presence or absence of a protein in cilia was analyzed to define ciliary targeting

Journal of Cell Science

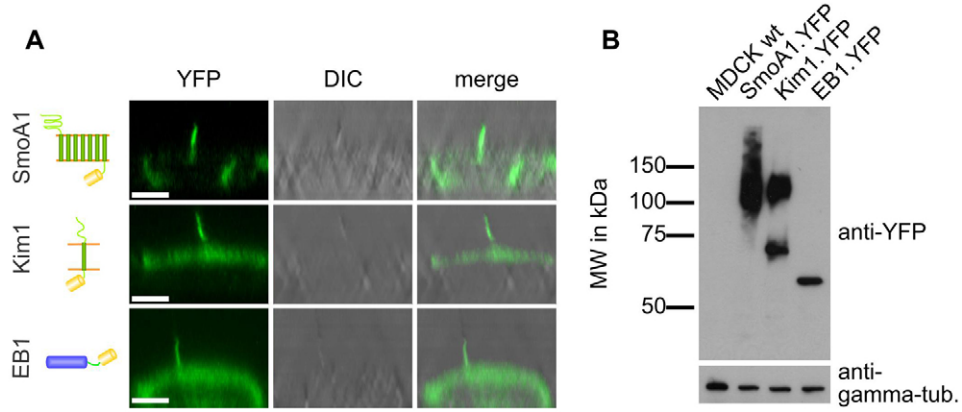

Fig. 1. Structure and localization pattern of the selected ciliary proteins. (**A**) SmoA1 is a seven-pass transmembrane protein. Kim1 is a single transmembrane protein with a short intracellular domain. EB1 is a cytosolic microtubule-associated protein. All proteins were fused to YFP at their C-terminus. Z-stack reconstructions of live MDCK cells, stably expressing SmoA1-, Kim1- or EB1-YFP fusion proteins. The fusion proteins are located at the primary cilium. In addition, SmoA1 is present basolaterally, Kim1 is localized at the apical membrane and EB1 diffusely in the cytosol. Scale bars: 5 µm. (**B**) Western blot showing expression of the YFP fusion proteins studied. Polyclonal MDCK cells expressing SmoA1-YFP, Kim1-YFP or EB1-YFP after retroviral transduction were lysed and equal protein amounts loaded onto a western gel. Blotting with YFP antibody shows roughly equal expression of the glycosylated SmoA1-YFP and Kim1-YFP and lower expression of EB1-YFP. Lysates from wild-type MDCK cells serve as a negative control. The gamma tubulin bands demonstrate equal loading. The 60 kDa band in the Kim1 lane is a lower glycosylated form (Bailly et al., 2002).

sequences or to characterize binary signaling switches (Corbit et al., 2005; Rohatgi et al., 2007). To overcome these limitations we developed a method based on fluorescence recovery after photobleaching (ciliary FRAP) to quantitatively compare the turnover of ciliary transmembrane proteins in renal epithelial-derived MDCK cells. Analyzing the role of Rab8, Rab5 and Rab23 on the ciliary transport of three different fluorescently tagged proteins with this technique, we confirm that transport to the cilium involves Rab8. Expression of dnRab5 slows the ciliary transport of the apical membrane protein Kim1 [kidney injury molecule-1; also known as hepatitis A virus cellular receptor 1 homolog (HAVCR1)] but does not alter the transport of Smoothened (Smo) or the end binding protein 1 (EB1; also known as microtubule-associated protein RP/EB family member 1). Interference with Rab23 by inducible expression of shRNA or a dominant negative mutant alters the ciliary steady state of Smo but not Kim1 or EB1, suggesting that Rab23 mediates the ciliary turnover of Smo and may possibly function in a recycling pathway.

Results

A FRAP-based method to compare the ciliary transport of fluorescently tagged ciliary proteins

To study the trafficking pathways of ciliary cargo molecules, we chose YFP coupled SmoA1, which localizes to the cilium

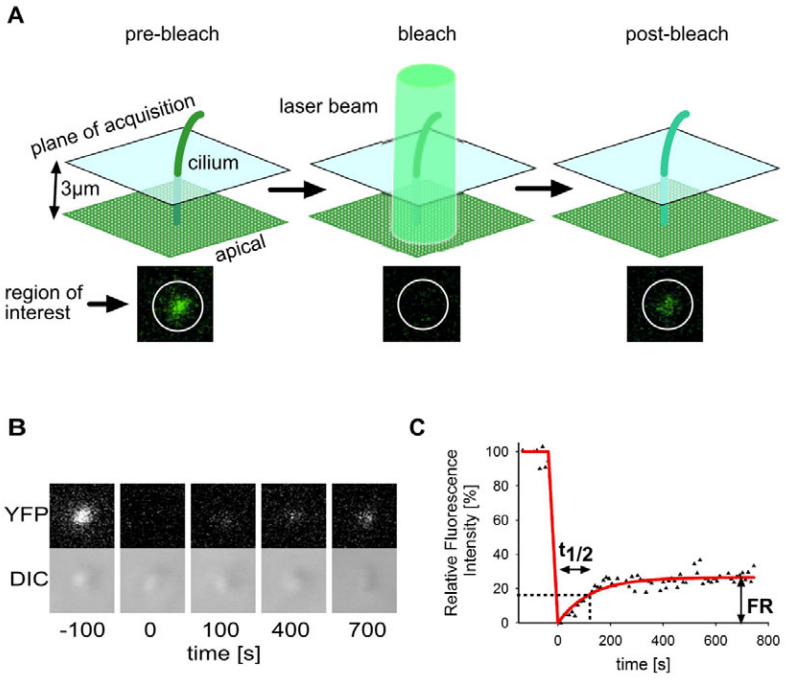

Fig. 2. Ciliary FRAP. (**A**) Experimental set-up. A 6×5 µm region surrounding the cilium was recorded 3 µm above the apical surface. After acquisition of pre-bleach images and high-power laser bleaching, a series of post-bleach images of the same region were acquired. The white circle indicates the measurement region for quantification of the fluorescence intensity in the cilium. (**B**) Ciliary FRAP experiment of a Kim1–YFP-expressing MDCK cell. The bottom panel is a DIC image showing the cilium. The upper panel shows the recovery of fluorescence in the ciliary region over a 700-second period. (**C**) Fitted recovery curve with the measured fluorescence intensities indicted by small triangles. Recovery half-time ($t_{1/2}$) and fraction recovered (FR) are indicated.

independently of hedgehog (HH) signaling (Xie et al., 1998), and the type 1 transmembrane molecule kidney injury molecule-1 (Kim1; Fig. 1A), a functional interactor of polycystin 2 involved in ciliary calcium signaling (Kotsis et al., 2007). MDCK cells were transduced by a retrovirus to create polyclonal cell lines stably expressing SmoA1 or Kim1 fused to YFP (Fig. 1B). SmoA1-YFP was expressed in the cilium and at the basolateral membrane, whereas Kim1-YFP was expressed in the cilium and the apical membrane (Fig. 1A). To study the transport dynamics of these receptors into the cilium, we developed a protocol based on fluorescence recovery after photobleaching (FRAP) (Reits and Neefjes, 2001) (Fig. 2). After bleaching the cilium by repetitive laser pulses (Fig. 2A), which eliminated all fluorescence in the cilium (Fig. 3), fluorescence recovery in the cilium was monitored over time in a plane 3 µm above the apical surface (Fig. 2A,B). Protein transport into the cilium was analyzed by two parameters – fraction recovered (FR) and recovery half-time ($t_{1/2}$; Fig. 2C). Since most ciliary proteins are mobile and turned over by ante- and retrograde IFT, we interpreted the FR to represent new molecules recruited to the ciliary compartment (see Fig. 4A,B for a schematic representation). The recovery half-time is inversely proportional to the delivery speed of fluorescent (unbleached) molecules to the cilium (Fig. 4B). Fig. 4C,D shows the recovery kinetics for SmoA1-YFP and Kim1-YFP. The FR of the two transmembrane receptors was much lower (SmoA1-YFP: 14%, Kim1-YFP: 31%) than that of End binding protein-1 (EB1: 66%; Fig. 1A,B and Fig. 4E), which is a non-membrane bound protein that is transported to the microtubular plus-ends at the ciliary tip (Pedersen et al., 2003). According to our model the lower FR of SmoA1 and Kim1 compared with EB1 could be explained by a higher recycling rate of bleached SmoA1 or Kim1 within the cilium. The recovery half-time was also markedly different between SmoA1 and Kim1 (41.3 seconds versus 73.3 seconds), and much slower than for EB1 (14.7 seconds; Fig. 4C-E), suggesting that differences in the mode of protein delivery to the ciliary compartment may exist.

Expression of dominant-negative Rab8a slows fluorescence recovery at the cilium

Rab8 has been described to act in conjunction with a complex of BBS proteins to transport cargo into the ciliary compartment (Nachury et al., 2007). We tested if interference with the function of Rab8 in our system affects the fluorescence recovery of ciliary proteins. The endogenous activity of Rab GTPases can be suppressed by exogenous expression of a mutated Rab that is locked in the GDP binding state, acting as a dominant-negative suppressor of the endogenous protein (Moritz et al., 2001). Since loss of Rab8a function interferes with ciliogenesis we adapted a lentivirus-encoded, tetracycline-inducible system (Wiznerowicz and Trono, 2003) that allowed the expression of dominant-negative (dn) Rab8a (T22N) fused to CFP in ciliated MDCK cells (Fig. 5A; for details see the Materials and Methods section). Interestingly, whereas wild-type Rab8a was present in the cilium (data not shown), this was not the case for Rab8a.T22N (Fig. 5B), suggesting that GTP-binding of Rab8 is necessary for transport to the cilium. Induction of Rab8a.T22N caused an increase in the $t_{1/2}$ of SmoA1 (70.3 seconds versus 41.3 seconds; $P<0.01$; Fig. 5C,D), but no significant difference was seen in the fraction recovered (Fig. 5E). Similar findings were observed when the effect of dnRab8a was analyzed on the FRAP characteristics of Kim1-YFP and EB1-YFP (Fig. 5F,G). This is in agreement with previous observations that Rab8 plays a central role in transporting

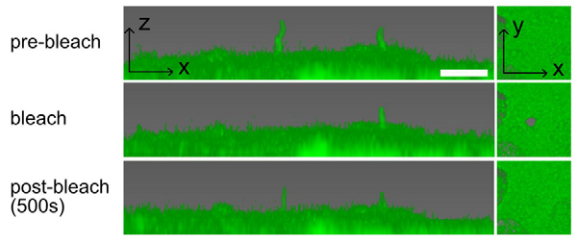

Fig. 3. Three-dimensional reconstruction in Imaris of a ciliary FRAP experiment with Kim1–YFP-expressing MDCK cells. The long panels on the left show an xz view of the apical membrane with two cilia before bleaching (pre-bleach). The xy panel on the right shows a view from the top onto the apical membrane. Bleaching of the left cilium (bleach) results in complete disappearance of fluorescence from the cilium. In the xy plane the bleached area is seen as a circular defect in the apical membrane. Recovery of fluorescence is seen in the left cilium after 500 seconds (post-bleach). Scale bar: 5 µm.

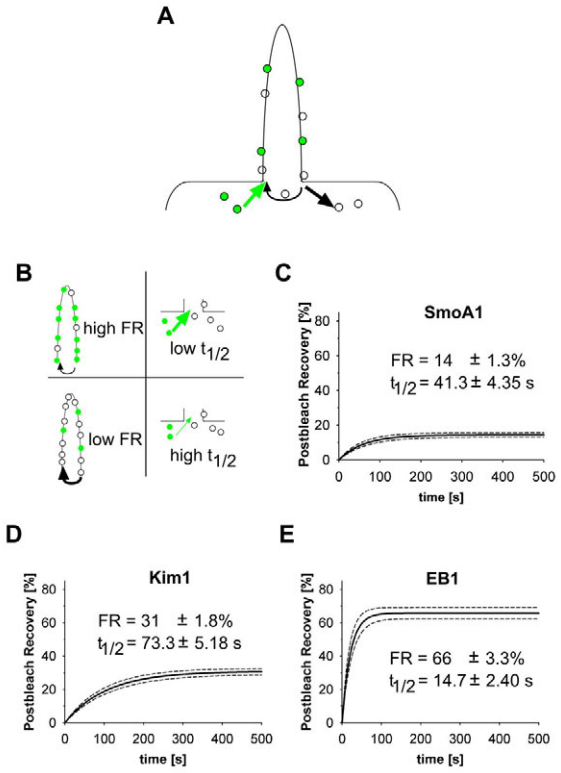

Fig. 4. Different ciliary proteins exhibit varied recovery kinetics in ciliary FRAP experiments. (**A**) A diagram showing how the fluorescence recovery of a protein in the cilium is determined by the amount of recycling of bleached protein (white circles, black curved arrow) and the delivery speed of unbleached protein (green circles and arrow). (**B**) A diagram of how a high FR, indicated by a large number of unbleached molecules (green), reflects low amounts of recycling. High amounts of recycling result in many bleached molecules (white circles) and a low FR. High delivery speed of unbleached protein (thick green arrow) results in fast recovery and low $t_{1/2}$. Slow recovery (thin arrow) results in high $t_{1/2}$. (**C-E**) FRAP curves for the different ciliary proteins. The solid line is the fitted curve; the dotted lines show ±1 s.e.m. The FRAP curves differ for all three proteins in respect to half-time recovery ($t_{1/2}$) and fraction recovered (FR).

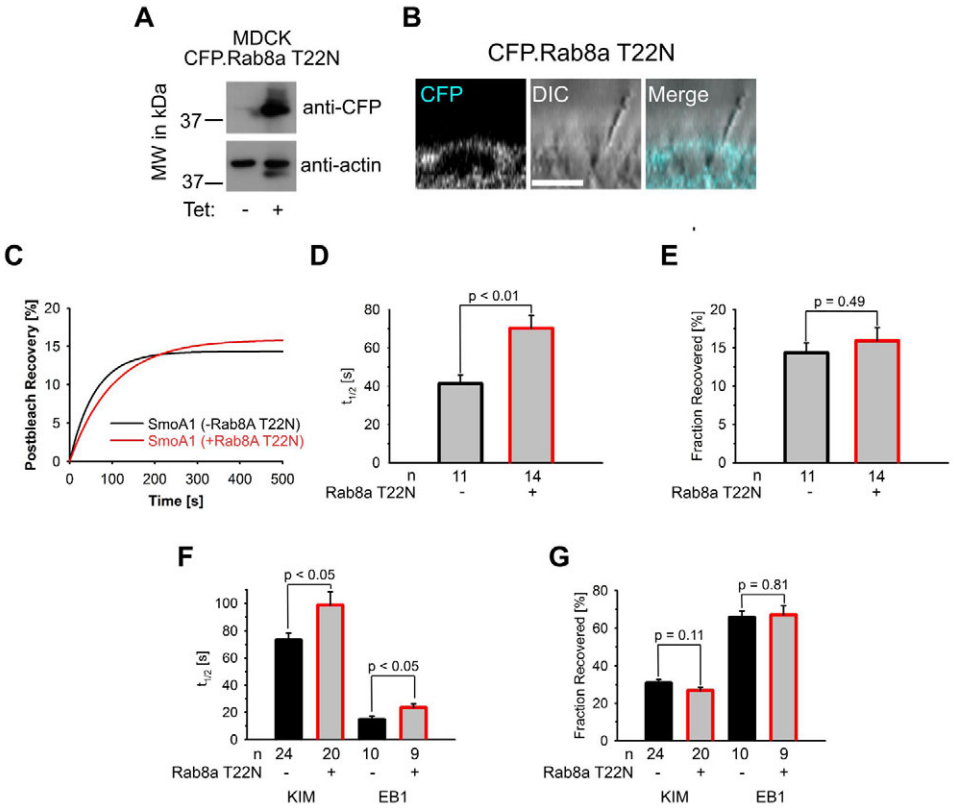

Fig. 5. Rab8 mediates protein transport into the cilium. (**A**) SmoA1–YFP-expressing MDCK cells were lentivirally transduced to express a tetracycline-sensitive repressor and CFP-coupled dnRab8a(T22N) under the control of a tet operator. Exposure of ciliated cells to tetracycline for 3 days resulted in strong expression of the mutant Rab8a (right lane). The actin bands demonstrate equal loading. SmoA1-YFP expression is not shown. (**B**) dnRab8a(T22N) is not present in the cilium. Scale bar: 5 µm. (**C**) The FRAP curve after induction of dnRab8 shows slower FRAP of SmoA1-YFP (red curve). (**D**) The $t_{1/2}$ for SmoA1 is significantly increased after induction of dnRab8a (for details see text). (**E**) No significant difference is seen in FR. (**F**) The $t_{1/2}$ for Kim1-YFP and EB1-YFP is significantly increased after induction of dnRab8a: Kim1: 98.6±9.82 seconds versus 73.3±5.18 seconds and EB1: 23.6±2.87 seconds versus 14.7±2.40 seconds. (**G**) Expression of dnRab8a has no significant influence on FR: Kim1: 27±1.6% versus 31±1.8%; EB1: 67±4.7% versus 66±3.3%.

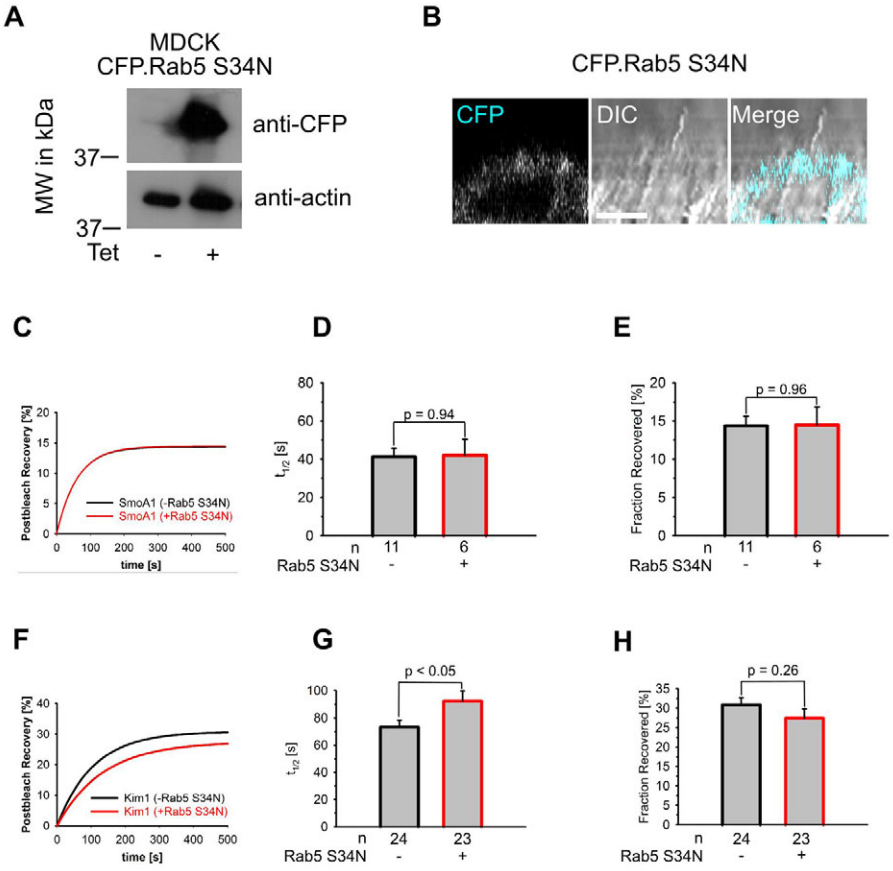

Fig. 6. Expression of dnRab5 slows the cFRAP characteristics of Kim1, but not of SmoA1. (**A**) SmoA1–YFP- or Kim1–YFP-expressing cells were transduced to express tetracycline inducible CFP-Rab5(S34N). Lysates obtained after 72 hours of exposure to tetracycline (+tet) show strong expression of dnRab5, whereas no expression is seen in the absence of tetracycline (–tet). (**B**) Z-stack of a ciliated CFP-Rab5(S34N)-expressing cell. A median filter was used. (**C-E**) The FRAP characteristics of SmoA1. (**C**) The FRAP curve for SmoA1-YFP is unchanged after expression of dnRab5 (red curve). (**D**) No significant difference is seen in $t_{1/2}$ of SmoA1 after expression of dnRab5: 42.0±8.44 seconds versus 41.3±4.35 seconds. (**E**) No significant difference is seen in FR of SmoA1: 14±2.3% versus 14±1.3%. (**F-G**) The FRAP characteristics of Kim1-YFP. (F) There is a markedly slower recovery of Kim1-YFP after expression of dnRab5 (red curve). (G) Quantification of $t_{1/2}$ shows a significant increase (92.3±7.51 seconds versus 73.3±5.18 seconds). (**H**) No significant change is seen in the FR after expression of dnRab5 (27±2.4% versus 31±1.8%).

cargo to the primary cilium (Moritz et al., 2001; Nachury et al., 2007; Yoshimura et al., 2007).

To exclude the possibility that these differences in the FRAP kinetics of ciliary cargo proteins were due to our expression system, or tetracycline, we created cells stably expressing SmoA1-, Kim1- or EB1-YFP and tetracycline-inducible dnRab5 (S34N). We did not expect EB1 transport to be affected by dnRab5, since Rab5 acts in the endocytic pathway from the apical membrane (Hoekstra et al., 2004) where EB1 is not present. When dnRab5 was induced in SmoA1-expressing cells in the same manner as dnRab8a (Fig. 6A,B), the recovery dynamics were unchanged (Fig. 6C-E) suggesting that Rab8 is involved in the ciliary transport of SmoA1, whereas Rab5 is not. These results are consistent with a recent report that failed to detect an association of Smo with endosomal markers (Wang et al., 2009). Similarly, expression of dnRab5 did not significantly change the recovery dynamics of EB1 (supplementary material Fig. S1A-C). However, expression of dnRab5 in Kim–YFP-expressing cells significantly slowed ciliary recovery after bleaching (Fig. 6F-H), suggesting that ciliary targeting of Kim1 involves recycling from the apical membrane and demonstrating that different pathways exist for the delivery of proteins to the ciliary compartment.

Loss of Rab23 function increases the fractional recovery of ciliary Smoothened

Rab23 has been implicated as a negative regulator of HH signaling, causing neural tube closure defects in knock-out animals (Eggenschwiler et al., 2006). Furthermore, Rab23 was identified in a screen as one of three Rab proteins necessary for ciliogenesis in immortalized retinal cells (Yoshimura et al., 2007). Currently it is not known how Rab23 is involved in HH signaling. We were interested to know whether interference with Rab23 function affects the transport kinetics of SmoA1 in the cilium. Analogous to Rab8, we found that wild-type Rab23 is localized in the cilium,

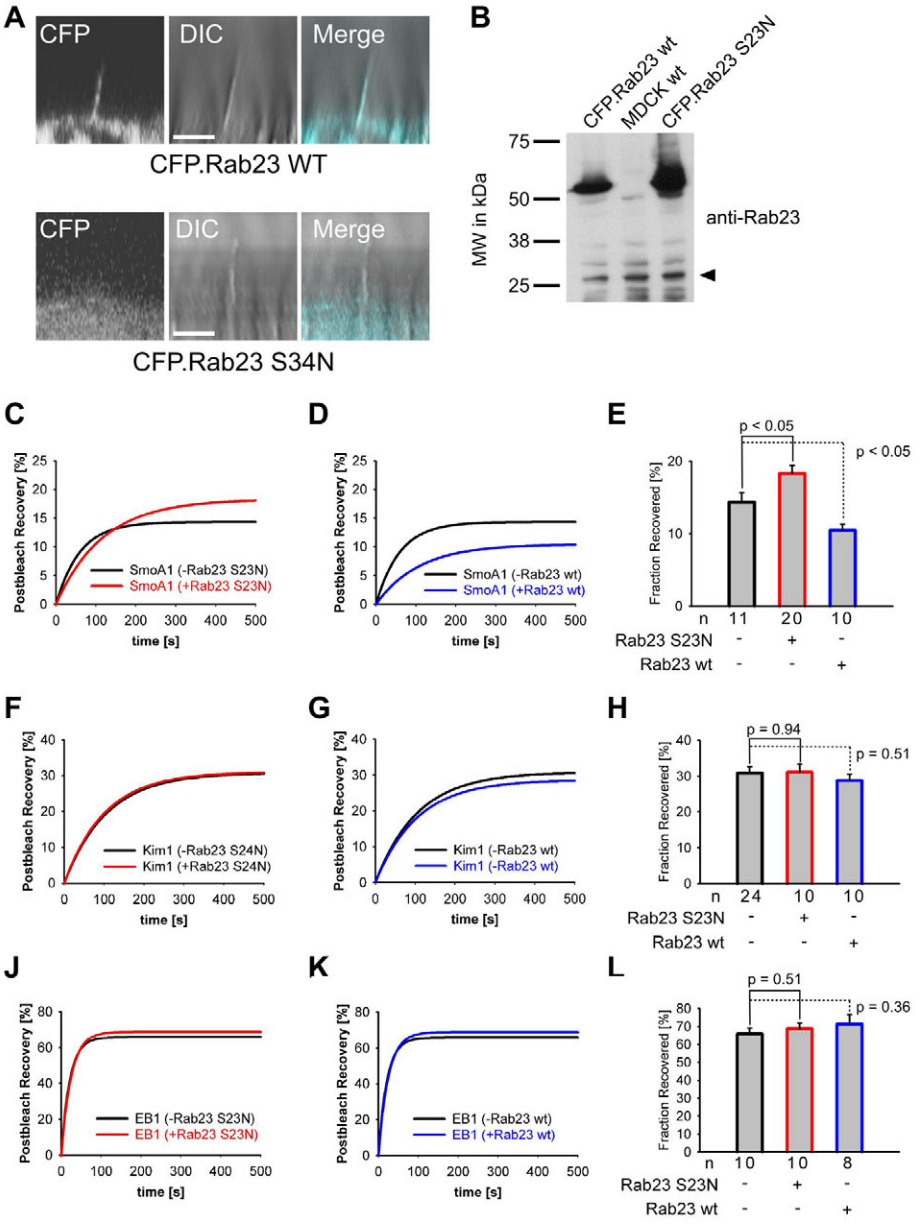

Fig. 7. Rab23 is localized in primary cilia and influences the ciliary kinetics of Smo. (**A**) Wild-type Rab23 was expressed in ciliated MDCK cells by tetracycline induction and was found to be localized in the cilium, but the dominant negative form was not. Scale bars: 5 µm. (**B**) Western blot depicting the expression of dominant-negative CFP-Rab23(S23N) and wild-type CFP-Rab23 compared with endogenous Rab23. Lysates of SmoA1-YFP MDCK cells expressing tetracycline inducible CFP-Rab23(S23N) or CFP-wtRab23 were analyzed after incubation with tetracycline for 72 hours. Blotting with anti-Rab23 antibody demonstrates several-fold higher expression of the induced proteins compared with endogenous Rab23 (arrowhead). SmoA1-YFP expression is not shown on this blot. (**C-E**) Rab23 modulates the fractional recovery of SmoA1. (C) Induced expression of dnRab23(S23N) results in increased FR of SmoA1 (red curve). (D) Induced expression of wild-type Rab23 results in decreased FR of SmoA1 (blue curve). (E) Quantification shows significantly increased FR after induction of dnRab23 (red framed bar) and decreased FR after induction of wtRab23 (blue framed bar). For details see text. (**F-L**) Rab23 does not modulate the fractional recovery of Kim1 or EB1. (F,J) Induced expression of dnRab23(S23N) results in unchanged FR of Kim1 (31±1.9% versus 31±1.8%) or EB1 (69±3.1% versus 66±3.3%; red curves). (G,K) Induced expression of wild-type Rab23 results in almost unchanged FR of Kim1 (29±2.2% versus 31±1.8%) and EB1 (71±5.3% versus 66±3.3%; blue curves). (H,L) Quantification shows no significant change in the FR after induction of dnRab23 (red framed bar) or after induction of wtRab23 (blue framed bar).

but not the GDP-bound form Rab23.S23N (Fig. 7A). Strikingly, while neither the induction of dnRab5 or dnRab8a had an impact on the FR of SmoA1 (Fig. 5E,G and Fig. 6H), induction of dnRab23 (S23N; Fig. 7B) significantly increased the FR of SmoA1 (Fig. 7C,E; 18% versus 14%, $P<0.05$). However, no significant differences were observed in the FR of Kim1 or EB1 after expression of dominant negative Rab23 (Fig. 7F,H,J,L), suggesting that the effect of dnRab23 is specific for SmoA1. Conversely, the induction of wild-type Rab23 decreased the FR of SmoA1 (Fig. 7B,D,E; 10% versus 14%, $P<0.05$), but not of Kim1 (Fig. 7G,H) or EB1 (Fig. 7K,L). To verify the effect of loss of Rab23 function on SmoA1 recovery by an independent approach we used lentiviral transduction to create SmoA1-YFP MDCK cells with tetracycline-inducible shRNA against Rab23, employing the same strategy as in the cells with inducible overexpression of dominant-negative Rab proteins. Exposure of these cells to tetracycline resulted in efficient knock-down of Rab23 and expression of a CFP reporter (Fig. 8A). When these cells were analyzed after tetracycline induction by ciliary FRAP we found a significant increase in the fraction recovered, compared with cells without tetracycline (15% versus 10%; $P<0.05$; Fig. 8B,C), thus recapitulating the results obtained after expression of dominant negative Rab23.

SmoA1 is an oncogenic variant of Smo that differs from wild-type Smo by its constitutive translocation to the cilium in the absence of HH stimulation, which possibly indicates different trafficking. Therefore, we tested whether Rab23 affects the ciliary levels of wild-type Smo. We analyzed the ciliary recovery of wild-type Smo-YFP after stimulation with ShhN-conditioned medium (supplementary material Fig. S2) by FRAP in the presence or absence of dnRab23. Analogous to the experiment using SmoA1-YFP the fraction of wild-type Smo recovered was significantly greater after expression of dnRab23 compared with the absence of dnRab23 (22% versus 17%, $P<0.05$; Fig. 8D,E). These results demonstrate that Rab23 affects the ciliary levels of SmoA1 as well as wild-type Smo.

In summary, our results on Rab23 suggest that loss of Rab23 function increases the fraction of recovered fluorescently tagged Smo in the cilium, but not of Kim1 or EB1, whereas increasing Rab23 has the opposite effect. According to our model this suggests that Rab23 functions to increase the recycling of bleached Smo and to allow the entry of less fluorescent (unbleached) protein into the ciliary compartment.

Discussion

In this work we used a new tool based on fluorescence recovery after photobleaching (FRAP) to study the dynamics of protein transport into the primary cilium of polarized epithelial cells. Previous studies relied on ciliogenesis or on the presence or absence of a protein to analyze ciliary trafficking pathways (Corbit et al., 2005; Nachury et al., 2007; Rohatgi et al., 2007; Yoshimura et al., 2007). By contrast, ciliary FRAP allows the tracking of ciliary cargo proteins not required for ciliary structure or function. Our study shows differing functions for Rab8, Rab5 and Rab23 in ciliary transport (Fig. 9). Rab8 is involved in the transport of all three studied proteins into the cilium, but Rab5 only plays a role in the trafficking of the apical-membrane-localized Kim1, but not of Smo or EB1. Importantly, we show that the ciliary kinetics of the HH pathway receptor Smo are influenced by alterations of Rab23 activity in a manner that is compatible with a putative role in protein recycling.

The basic steps of intraflagellar transport have been well characterized (Pedersen et al., 2008). The kinesin II motor carries IFT proteins, dynein 2 and other cargo molecules from the base of the cilium to the tip. There the complexes are rearranged and dynein 2 transports IFT proteins and cargo back to the base where the proteins are thought to be released into the cytoplasm for recycling. In light of this paradigm we suggest that the amount of non-recovered fluorescence represents recycled protein that is bleached, whereas the recovered fluorescence represents unbleached protein from outside the bleached cilium and basal body compartment (see Fig. 3 for a schematic model). According to this model the speed of fluorescence recovery is determined by the rate of protein entry into the cilium and is independent of the protein transport rate within the cilium. We cannot exclude the possibility that a part of the non-recovered fluorescence is due to protein that has uncoupled from IFT and is stationary within the ciliary membrane. Uncoupling, however, has not been reported, and recent evidence suggests that Smo is transported in the cilium together with IFT molecules (Wang et al., 2009).

The mechanism by which proteins are shuttled to the ciliary compartment is beginning to emerge: in the photoreceptor, Rab6, -8 and -11 are involved in vesicular trafficking to the base of the cilium, where vesicles fuse with the membrane, allowing cargo to access the ciliary membrane (Maerker et al., 2008; Papermaster et al., 1985). Recently it was shown in frog retina that Rab11 acts in concert with Arf4 to target rhodopsin and other proteins via specific

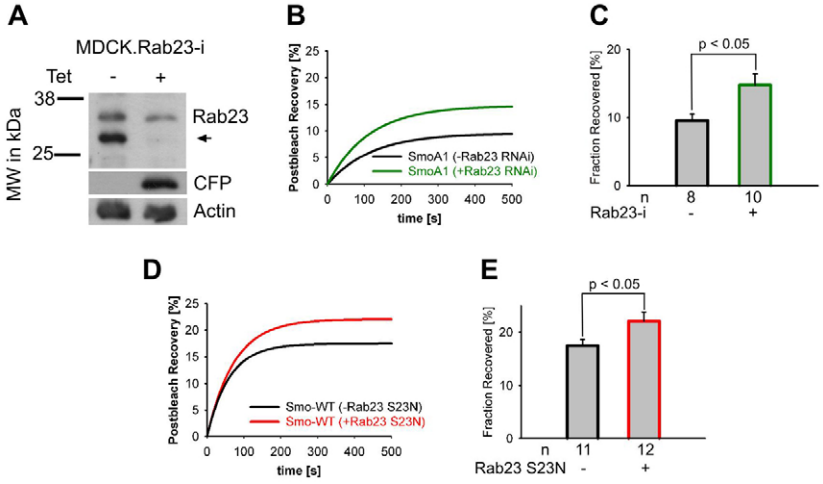

Fig. 8. SmoA1 and wild-type Smo are affected by loss of Rab23 function. (**A**) Western blot showing almost complete knock-down of endogenous Rab23 (arrow) and expression of a CFP reporter after 72 hours incubation with tetracycline. The actin bands demonstrate equal loading. (**B**) The knock-down of Rab23 after tetracycline induction results in a higher FR of SmoA1-YFP (green curve). Note that these curves were obtained with a different microscope. (**C**) Quantification shows a significantly higher FR after tetracycline induction of Rab23 RNAi. (**D**) Induced expression of dnRab23(S23N) results in an increased FR of wild-type Smo (red curve). (**E**) Quantification shows a significantly increased FR after induction of dnRab23 (red framed bar). For details see text.

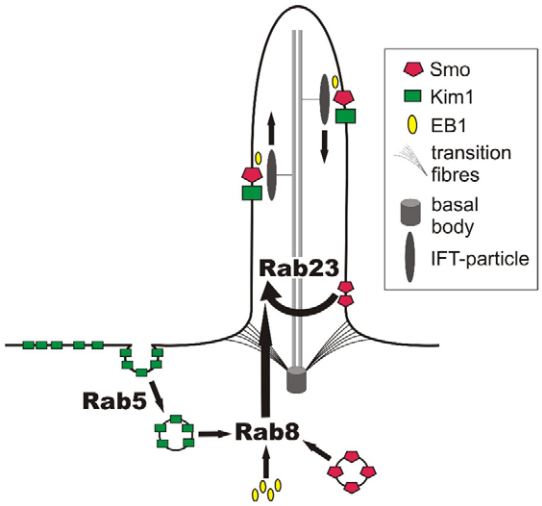

Fig. 9. A model for the role of different Rab proteins in protein transport to the cilium. Kim1 is localized at the apical membrane, where it is internalized via Rab5-mediated endocytosis and then delivered to the cilium via Rab8-mediated transport. EB1 enters the cilium in a Rab8-dependent manner, but independently of Rab5. Smo enters the ciliary compartment via Rab8. Upon exit from the cilium, Smo is recycled back by Rab23. Rab23-dependent transport is specific for Smo in respect to the three tested proteins.

N-terminal targeting sequences to the base of the cilium (Mazelova et al., 2009). In mammalian cells, a multimeric complex of BBS proteins recruits Rab8-containing vesicles via its GEF Rabin8 to the basal body region (Nachury et al., 2007). In agreement with these results the expression of dominant-negative Rab8 slowed the entry of all three proteins studied in our system. Expression of dnRab5 had no effect on the ciliary trafficking of Smo or EB1, but interestingly slowed the transport of Kim1, a protein expressed at the apical membrane. The finding that interference with endocytosis through expression of dnRab5 had no effect on the ciliary transport of Smo is in agreement with a recently published report that showed lateral movement of Smo from the plasma membrane to the cilium in the presence of dominant negative dynamin (Milenkovic et al., 2009). Interestingly, our results show a different scenario for the apical protein Kim1 whose ciliary localization is delayed after interference with endocytic transport. These data strongly suggest that more than one pathway exists to recruit ciliary proteins from the apical membrane to the cilium. Rab5 has so far not been involved in ciliary protein transport. In a screen of multiple different Rab proteins, Rab5 was not associated with ciliogenesis (Yoshimura et al., 2007). Consistent with this observation, knock-down of Kim1 does not disturb cilia formation (data not shown), which might indicate that Rab5 is not involved in the transport of proteins required for ciliogenesis.

No data exist on how cilia proteins are recycled back, once they exit the ciliary compartment. Interestingly, we found that interference with Rab23 function through expression of dominant-negative Rab23 or shRNA-mediated knock-down specifically increased the amount of new Smo protein in the cilium. This differs from the effect of dominant-negative Rab8 and -5, for which the recovery half time, but not the amount of recovered fluorescent protein was altered. By applying our model of ciliary recycling we believe that Rab23 might function to recycle Smo back into the cilium. Interference with this function would lead to a decreased steady-state of Smo and explain the increased entry of unbleached protein into the cilium.

It is interesting that the effect of Rab23 in our study was specific for Smo. Rab23 has been identified as a negative regulator of sonic hedgehog signaling (Eggenschwiler et al., 2006). Inactivation of Rab23 in mice results in the open brain phenotype, caused by ventralization during neural development, indicative of un-opposed HH signaling. The underlying mechanism is unclear and our study was not designed to address the mechanism of how Smo recycling affects HH signaling, but our results implicate Rab23 in the ciliary trafficking of Smo, and for the first time show a possible mechanism of how Rab23 may function in the HH pathway. Future studies will need to identify whether specific recycling pathways exist for other ciliary cargo.

Materials and Methods

Reagents

Polyclonal rabbit anti-GFP antibodies were obtained from MBL International (Woburn, MA, USA), monoclonal mouse anti-β-actin, and anti-acetylated tubulin antibodies, and tetracycline were obtained from Sigma (Taufkirchen, Germany). Anti-Rab23 was obtained from ProteinTech Group (Chicago, IL, USA). Anti-Shh was obtained from Cell Signaling (Boston, MA, USA). Baysilone was obtained from GE Bayer Silicones (Leverkusen, Germany).

Constructs and plasmids

The oncogenic variant of mouse Smoothened, SmoA1, was obtained from A. Dlugosz (Taipale and Beachy, 2001), subcloned into pLXSN in frame with C-terminal Venus, a variant of the yellow fluorescent protein (YFP) (Nagai et al., 2002). pLV-TH and pLV-tTRKRAB-Red were obtained from Didier Trono (Wiznerowicz and Trono, 2003). pLV-TH was modified by silencing *Xho*I restriction sites at positions 3087 and 5086, a *Not*I restriction site at position 1146, and introduction of *Mlu*I and *Not*I sites between the resulting unique *Xho*I and *Spe*I sites. Wild-type or dominant-negative Rab proteins were cloned into the *Mlu*I and *Not*I sites with the Cyan fluorescent protein (CFP) variant Cerulean (Rizzo et al., 2004) as an N-terminal fusion. shRNA constructs against canine Rab23 were screened and an effective shRNA construct cloned into a modified pLVTH vector carrying a CFP reporter as described previously (Kottgen et al., 2008). The target sequence for Rab23-i is 5′-GCGACAAATCCAAGTTAAT-3′. Canine Rab5 and Rab8A were obtained from Marino Zerial and Kai Simons (Chavrier et al., 1991) and murine Rab23 from Carol Wicking (Evans et al., 2003).

Cell culture and protein analysis

ShhN-conditioned medium was produced by transfecting HEK293T cells with 10 μg of pcDNA3::ShhN using 250 mM CaCl. Conditioned medium was harvested 48 hours post-transfection, pooled, filtered through a 0.2 μm PES syringe filter (Millipore), and buffered with 5 mM Hepes, pH 7.5. SDS-PAGE and western blot analysis were performed as described previously (Kuehn et al., 2007). MDCK II cells, expressing Cerulean-tagged proteins were kept in Dulbecco's modified Eagle's medium (DMEM) + 10% FBS, and 1% penicillin-streptomycin. MDCK II cells expressing Venus fusion proteins were maintained in DMEM + 10% FBS, 1% penicillin-streptomycin, and 2.5 mg/ml of G418. MDCK cells were grown to confluence on 30 mm glass coverslips for 10 days for optimal cilia outgrowth. Lentiviral production was performed as described previously (Wiznerowicz and Trono, 2003). Retroviral production and transfection of target cells were performed as described previously (Kotsis et al., 2007). Polyclonal cell-lines coexpressing different transgenes were produced by sequential retro- or lentiviral gene transfer. For the conditional expression of Cerulean-tagged Rab GTPases, or Rab23 shRNA MDCK cells were co-transduced with pLV-tTRKRAB-Red. Expression of the Rab proteins in ciliated cells was induced by 5 μg/ml tetracycline for 72 hours.

Confocal laser microscopy

For laser scanning microscopy, MDCK cells were loaded in an open perfusion chamber, layered with Ringer's solution, and analyzed using a laser scanning microscope LSM 510 Meta equipped with a Plan Neofluar ×100/1.3 NA oil objective (both from Carl Zeiss MicroImaging, Jena, Germany). Excitation of the fluorophores (Cerulean and Venus) was performed at 458 and 514 nm, respectively. For detection of the emission signal the spectral Meta detector was used, collecting the light in the range 462-512 nm for the Cerulean fusion proteins, and 516-623 nm for the Venus fusion proteins. Image analysis and three-dimensional reconstruction were performed using Imaris 5.0 (Bitplane, Zurich, Switzerland). Experiments with Rab23-i were performed with the LSM5 LIVE laser scanning microscope with a Plan Neofluar ×100/1.3 NA oil objective (software 4.0; Carl Zeiss MicroImaging, Jena, Germany).

Image acquisition in live MDCK cells and time-series experiments

Cells were washed before the experiment with 1 ml of CO_2-independent Ringer's solution (145 mM NaCl, 0.4 mM K_2HPO_4, 1.6 mM KH_2PO_4, 5 mM glucose, 1 mM

$MgCl_2$, 1.3 mM calcium gluconate) and pre-warmed to 37°C. Excess liquid on the coverslip was blotted with a filter paper. The coverslip was mounted onto the bottom of an open plastic chamber (cell-layer side facing upwards), covered with Baysilone, followed by the addition of 1 ml of pre-warmed Ringer's solution. The open chamber was then placed onto a water-heated stage providing constant temperature in the open chamber (37°C). To minimize focus shifts, the cells were incubated on the heating stage for 30 minutes before image acquisition started.

Fluorescence recovery after photobleaching (FRAP)

See also Fig. 2. FRAP recordings were carried out in CO_2-independent Ringer's solution. The acquisition plane was set 3 µm above the apical surface. The region of acquisition was adjusted to 6×5 µm, pixel size 0.04 µm, pixel time 2.56 µseconds, (wavelength 514 nm). Images were stored with 12-bit grayscale resolution. The 2.4 µm diameter photobleaching area (20 repetitive pulses, wavelength 514 nm) included the ciliary shaft (Fig. 3). An autofocus routine using the coverslip reflex at 633 nm was performed every 100 seconds to correct the vertical position of the cell. Time series were recorded under the control of the MultiTime 3.0 macro (Carl Zeiss MicroImaging GmbH, Jena, Germany).

Image analysis and statistics

For quantification of the ciliary FRAP experiments, acquired images were exported to the Tiff file format. Fluorescence intensity in the cilium was measured using Metamorph software (version 6.26, Molecular Devices, Downingtown, USA). The circular measurement region was set to 1.2 µm diameter; and the center of the measurement region was adjusted according to the coordinates of the cilium as determined in the DIC image at the same time-point. The average intensity of the image was subtracted at each time point as background. Recovery intensities as a function of time were fit to an exponential curve, described by the following equation: $I(t)=I_E(1-e^{-\tau t})$, where I is intensity, I_E is maximum intensity, t is time and τ is an intermediate variable. I_E was identical to the fraction recovered (FR), and τ was used to calculate a recovery half-time ($t_{½}$), by the following equation: $t_{½}=\ln 0.5/-\tau$. Fitting was done using SigmaPlot software (Systat Software GmbH, Erkrath, Germany). Qualitative analysis of the resulting curves was performed based on the coefficient of determination (R^2). Only experiments with $R^2>0.6$ were included into the statistical analysis. If this cut-off yielded more than 25 experiments, $R^2>0.65$ was used as a threshold. The fluorescence recovery curves were calculated from the averaged experimentally determined values. Statistical analysis of FR and $t_{½}$ was performed in Microsoft Excel (Microsoft Corporation). Statistical comparisons were done by unpaired, two tailed t-test. $P<0.05$ was considered statistically significant. Error bars represent standard error of the mean (s.e.m.).

We thank K. Simons (Max Planck Institute of Molecular Cell Biology and Genetics, Dresden, Germany) for the Rab8a construct, M. Zerial (Max Planck Institute of Molecular Cell Biology and Genetics, Dresden, Germany) for the Rab5 construct, C. Wicking (University of Queensland, St Lucia, Australia) for the Rab23 construct, A. Dlugosz (University of Michigan, Ann Arbor, MI, USA) for SmoA1, J. Reiter (University of California, San Francisco, CA, USA) for the wild-type Smo and P. Chuang (University of California, San Francisco, CA, USA) for the ShhN construct. We thank Simone Braeg for expert technical assistance and members of the Walz lab for helpful discussions. This work was funded by the DFG (E.W.K.), FP7 Eucilia project, grant no. HEALTH-F2-2007-201804 (G.W.), SFB 592 project Z2 (R.N.), and by the Excellence Initiative of the German Federal and State Governments (EXC 294).

Supplementary material available online at
http://jcs.biologists.org/cgi/content/full/123/9/1460/DC1

References

Bailly, V., Zhang, Z., Meier, W., Cate, R., Sanicola, M. and Bonventre, J. V. (2002). Shedding of kidney injury molecule-1, a putative adhesion protein involved in renal regeneration. *J. Biol. Chem.* **277**, 39739-39748.

Chavrier, P., Gorvel, J. P., Stelzer, E., Simons, K., Gruenberg, J. and Zerial, M. (1991). Hypervariable C-terminal domain of rab proteins acts as a targeting signal. *Nature* **353**, 769-772.

Corbit, K. C., Aanstad, P., Singla, V., Norman, A. R., Stainier, D. Y. and Reiter, J. F. (2005). Vertebrate Smoothened functions at the primary cilium. *Nature* **437**, 1018-1021.

Deretic, D. (1997). Rab proteins and post-Golgi trafficking of rhodopsin in photoreceptor cells. *Electrophoresis* **18**, 2537-2541.

Eggenschwiler, J. T., Bulgakov, O. V., Qin, J., Li, T. and Anderson, K. V. (2006). Mouse Rab23 regulates hedgehog signaling from smoothened to Gli proteins. *Dev. Biol.* **290**, 1-12.

Evans, T. M., Ferguson, C., Wainwright, B. J., Parton, R. G. and Wicking, C. (2003). Rab23, a negative regulator of hedgehog signaling, localizes to the plasma membrane and the endocytic pathway. *Traffic* **4**, 869-884.

Follit, J. A., Tuft, R. A., Fogarty, K. E. and Pazour, G. J. (2006). The intraflagellar transport protein IFT20 is associated with the Golgi complex and is required for cilia assembly. *Mol. Biol. Cell* **17**, 3781-3792.

Grosshans, B. L., Ortiz, D. and Novick, P. (2006). Rabs and their effectors: achieving specificity in membrane traffic. *Proc. Natl. Acad. Sci. USA* **103**, 11821-11827.

Hoekstra, D., Tyteca, D. and van IJzendoorn, S. C. D. (2004). The subapical compartment: a traffic center in membrane polarity development. *J. Cell Sci.* **117**, 2183-2192.

Kotsis, F., Nitschke, R., Boehlke, C., Bashkurov, M., Walz, G. and Kuehn, E. W. (2007). Ciliary calcium signaling is modulated by kidney injury molecule-1 (Kim1). *Pflugers Arch.* **453**, 819-829.

Kottgen, M., Buchholz, B., Garcia-Gonzalez, M. A., Kotsis, F., Fu, X., Doerken, M., Boehlke, C., Steffl, D., Tauber, R., Wegierski, T. et al. (2008). TRPP2 and TRPV4 form a polymodal sensory channel complex. *J. Cell Biol.* **182**, 437-447.

Kuehn, E. W., Hirt, M. N., John, A. K., Muehlenhardt, P., Boehlke, C., Putz, M., Kramer-Zucker, A. G., Bashkurov, M., van de Weyer, P. S., Kotsis, F. et al. (2007). Kidney injury molecule 1 (Kim1) is a novel ciliary molecule and interactor of polycystin 2. *Biochem. Biophys. Res. Commun.* **364**, 861-866.

Lin, F., Hiesberger, T., Cordes, K., Sinclair, A. M., Goldstein, L. S., Somlo, S. and Igarashi, P. (2003). Kidney-specific inactivation of the KIF3A subunit of kinesin-II inhibits renal ciliogenesis and produces polycystic kidney disease. *Proc. Natl. Acad. Sci. USA* **100**, 5286-5291.

Maerker, T., van Wijk, E., Overlack, N., Kersten, F. F., McGee, J., Goldmann, T., Sehn, E., Roepman, R., Walsh, E. J., Kremer, H. et al. (2008). A novel Usher protein network at the periciliary reloading point between molecular transport machineries in vertebrate photoreceptor cells. *Hum. Mol. Genet.* **17**, 71-86.

Mazelova, J., Ransom, N., Astuto-Gribble, L., Wilson, M. C. and Deretic, D. (2009). Syntaxin 3 and SNAP-25 pairing, regulated by omega-3 docosahexaenoic acid, controls the delivery of rhodopsin for the biogenesis of cilia-derived sensory organelles, the rod outer segments. *J. Cell Sci.* **122**, 2003-2013.

Milenkovic, L., Scott, M. P. and Rohatgi, R. (2009). Lateral transport of Smoothened from the plasma membrane to the membrane of the cilium. *J. Cell Biol.* **187**, 365-374.

Moritz, O. L., Tam, B. M., Hurd, L. L., Peranen, J., Deretic, D. and Papermaster, D. S. (2001). Mutant rab8 impairs docking and fusion of rhodopsin-bearing post-Golgi membranes and causes cell death of transgenic Xenopus rods. *Mol. Biol. Cell* **12**, 2341-2351.

Nachury, M. V., Loktev, A. V., Zhang, Q., Westlake, C. J., Peranen, J., Merdes, A., Slusarski, D. C., Scheller, R. H., Bazan, J. F., Sheffield, V. C. et al. (2007). A core complex of BBS proteins cooperates with the GTPase Rab8 to promote ciliary membrane biogenesis. *Cell* **129**, 1201-1213.

Nagai, T., Ibata, K., Park, E. S., Kubota, M., Mikoshiba, K. and Miyawaki, A. (2002). A variant of yellow fluorescent protein with fast and efficient maturation for cell-biological applications. *Nat. Biotechnol.* **20**, 87-90.

Papermaster, D. S., Schneider, B. G. and Besharse, J. C. (1985). Vesicular transport of newly synthesized opsin from the Golgi apparatus toward the rod outer segment. Ultrastructural immunocytochemical and autoradiographic evidence in Xenopus retinas. *Invest. Ophthalmol. Vis. Sci.* **26**, 1386-1404.

Pedersen, L. B., Geimer, S., Sloboda, R. D. and Rosenbaum, J. L. (2003). The Microtubule plus end-tracking protein EB1 is localized to the flagellar tip and basal bodies in Chlamydomonas reinhardtii. *Curr. Biol.* **13**, 1969-1974.

Pedersen, L. B., Veland, I. R., Schroder, J. M. and Christensen, S. T. (2008). Assembly of primary cilia. *Dev. Dyn.* **237**, 1993-2006.

Reits, E. A. and Neefjes, J. J. (2001). From fixed to FRAP: measuring protein mobility and activity in living cells. *Nat. Cell. Biol.* **3**, E145-E147.

Rizzo, M. A., Springer, G. H., Granada, B. and Piston, D. W. (2004). An improved cyan fluorescent protein variant useful for FRET. *Nat. Biotechnol.* **22**, 445-449.

Roepman, R. and Wolfrum, U. (2007). Protein networks and complexes in photoreceptor cilia. *Subcell. Biochem.* **43**, 209-235.

Rohatgi, R., Milenkovic, L. and Scott, M. P. (2007). Patched1 regulates hedgehog signaling at the primary cilium. *Science* **317**, 372-376.

Rosenbaum, J. L. and Witman, G. B. (2002). Intraflagellar transport. *Nat. Rev. Mol. Cell Biol.* **3**, 813-825.

Scholey, J. M. and Anderson, K. V. (2006). Intraflagellar transport and cilium-based signaling. *Cell* **125**, 439-442.

Singla, V. and Reiter, J. F. (2006). The primary cilium as the cell's antenna: signaling at a sensory organelle. *Science* **313**, 629-633.

Taulman, P. D., Haycraft, C. J., Balkovetz, D. F. and Yoder, B. K. (2001). Polaris, a protein involved in left-right axis patterning, localizes to basal bodies and cilia. *Mol. Biol. Cell* **12**, 589-599.

Taipale, J. and Beachy, P. A. (2001). The Hedgehog and Wnt signalling pathways in cancer. *Nature* **411**, 349-354.

Wang, Y., Zhou, Z., Walsh, C. T. and McMahon, A. P. (2009). Selective translocation of intracellular Smoothened to the primary cilium in response to Hedgehog pathway modulation. *Proc. Natl. Acad. Sci. USA* **106**, 2623-2628.

Wiznerowicz, M. and Trono, D. (2003). Conditional suppression of cellular genes: lentivirus vector-mediated drug-inducible RNA interference. *J. Virol.* **77**, 8957-8961.

Xie, J., Murone, M., Luoh, S. M., Ryan, A., Gu, Q., Zhang, C., Bonifas, J. M., Lam, C. W., Hynes, M., Goddard, A. et al. (1998). Activating Smoothened mutations in sporadic basal-cell carcinoma. *Nature* **391**, 90-92.

Yoder, B. K., Tousson, A., Millican, L., Wu, J. H., Bugg, C. E., Jr, Schafer, J. A. and Balkovetz, D. F. (2002). Polaris, a protein disrupted in orpk mutant mice, is required for assembly of renal cilium. *Am. J. Physiol. Renal Physiol.* **282**, F541-F552.

Yoshimura, S., Egerer, J., Fuchs, E., Haas, A. K. and Barr, F. A. (2007). Functional dissection of Rab GTPases involved in primary cilium formation. *J. Cell Biol.* **178**, 363-369.